Metastable room-temperature twist-bend nematic phases via photopolymerization

Nina Trbojevic,[1] Daniel J. Read,[2] and Mamatha Nagaraj[1,*]
[1]*School of Physics and Astronomy, University of Leeds, Leeds LS2 9JT, United Kingdom*
[2]*School of Mathematics, University of Leeds, Leeds LS2 9JT, United Kingdom*

(Received 20 March 2019; published 17 June 2019)

The heliconical twist-bend nematic (N_{TB}) phase is a promising candidate for novel electro-optic and photonic applications. However, the phase generally exists at elevated temperatures and across a narrow temperature interval, limiting its implementation in device fabrication, which would ideally require the liquid crystal phase to be stable at room temperature. Here we report the formation of room-temperature N_{TB} phases by *in situ* photopolymerization. A complete phase diagram of the liquid crystal and monomer mixtures is presented and the nature of the polymerized samples is discussed in detail. In contrast to samples before polymerization–where the N_{TB} phases exist at elevated temperatures and across temperature intervals of width $<10\,°C$–all photopolymerized N_{TB} samples are found to be stable at room temperature and exist over a temperature interval of up to 80 °C. Scanning electron microscopy of the polymerized N_{TB} phase shows that the polymer strands assemble at an angle with respect to the direction of the helical axis. This suggests that photopolymerized N_{TB} phases could be used to facilitate the tilt angle measurements in the twist-bend nematic phase.

DOI: 10.1103/PhysRevE.99.062704

I. INTRODUCTION

Liquid crystals are a fascinating class of optoelectronic materials that elegantly combine order and mobility. The twist-bend nematic (N_{TB}) phase is a liquid crystal phase that has attracted considerable attention due to (1) the possibility of achieving microsecond response times [1,2] when an external electric field is applied across the sample, and (2) the formation of spontaneously self-assembled nanoscale helical structures through simultaneous twisting and bending of the nematic director in space [3,4]. It is remarkable that the twisting and bending of the director occurs spontaneously, and overall the phase attains a structure where the local nematic director $\boldsymbol{n}$ lies at a "tilt" angle (θ) with respect to a helical axis (z), even though the constituent molecules that form the N_{TB} phase are achiral in nature. The N_{TB} director can be described as: $\boldsymbol{n} = (\sin\theta\cos\varphi,\ \sin\theta\sin\varphi,\ \cos\theta)$, where the azimuthal angle $\varphi = t_{TB}z$ and $t_{TB} = 2\pi/p_{TB}$ (p_{TB} is the pitch of the helix). For the N_{TB} phase, the tilt angle falls in the range $0 < \theta < \pi/2$, and obviously, in the case of the nematic phase, $\theta = 0$. The twist-bend nematic phase is exhibited by mesogens of various structures, including dimers [5–7], trimers [8,9], and bent-core liquid crystals [10,11]. With the exception of a trimeric [8] liquid crystal that consists of a combination of bent-core and rodlike components, the N_{TB} phase in all other materials exists at elevated temperatures, over a narrow temperature interval below the isotropic or nematic phases. It generally supercools to be metastable at room temperature and crystallizes within a few hours [12,13]. However, practical applications require materials that (1) are stable at room temperature, (2) exhibit the phase across a broad range of temperatures, and (3) can be readily made from commercially available precursors. One way of meeting these requirements is to thermodynamically stabilize the liquid crystal phase using mesogenic polymer networks. This can be achieved by mixing a small concentration of reactive bifunctional mesogenic monomer with low molecular weight liquid crystals that exhibit the required phase(s). An *in situ* photoinitiated polymerization fixes and stabilizes the anisotropic network and this process is usually referred to as "polymer stabilization" in literature. The general idea is to stabilize the orientation of the liquid crystal director (alignment) by nematic interactions between the aligned polymer network and the liquid crystal [14–16]. Polymer stabilization of liquid crystals provides an enhancement of mechanical stability and improved electro-optical characteristics.

In the past, photopolymerization has been successfully used to extend the temperature range and enhance electro-optic properties of nematic [17,18] and twist-grain boundary [19] phases. Polymer stabilization of blue phase liquid crystals leads to a vast array of practical photonic and display applications [20,21]. Polymer stabilization of cholesteric, [22–24] ferroelectric [25–28], and antiferroelectric [29] liquid crystal phases has also been achieved. In these systems, the formation of a polymer network in the lattice of disclinations provides thermal stability for the mesophases over a wide temperature range. Even though, in principle, such an approach could be used to extend the temperature range over which the N_{TB} phase is stable, it has not been reported so far. Photopolymerization of the N_{TB} phase was performed by Panov *et al.* [30] to demonstrate its usefulness in exploring complex hierarchical structures of the N_{TB} phase.

In this article, the formation of room-temperature N_{TB} phase via photopolymerization is presented. The formation of the N_{TB} phase in liquid crystal mixtures containing various mesogenic monomer concentrations, before polymerization, is discussed. The photopolymerized N_{TB} phases were kept

*m.nagaraj@leeds.ac.uk

under observation for a period of several months where they were found to remain stable (no crystallization). Hence, the N_{TB} phases are referred to as "metastable" in the paper. In the polymerized samples, the temperature range of the N_{TB} phase gets extended on both sides of the N-N_{TB} phase transition temperature of the corresponding mixture before polymerization, giving rise to the N_{TB} phases that exist over a temperature interval of up to 80 °C. Interestingly, in all of the polymerized samples, upon heating from the N_{TB} phase to the isotropic phase, residual birefringence is observed above the isotropic transition of the unpolymerized liquid crystal. SEM imaging of the photopolymerized N_{TB} phase shows that the polymer strands assemble at an angle corresponding to the tilt angle of the N_{TB} phase.

II. EXPERIMENTAL

The polymerizable mixtures consist of CB7CB [1,7-bis(4-cyanobiphenyl-4′-yl)heptane] (Synthon Chemicals), which exhibits nematic and N_{TB} phases, RM257 [4-(3-acryloyloxypropyloxy)benzoic acid 2-methyl-1,4-phenylene ester] (Synthon Chemicals), which is a monomeric liquid crystal exhibiting the nematic phase, and 0.5 wt% of photoinitiator benzoin methyl ether (Sigma Aldrich). Homemade planar antiparallel-rubbed cells were capillary filled with the polymerizable mixtures in the nematic phase. The samples were irradiated with UV light of 365 nm for 2 h to ensure complete polymerization, while maintaining a constant temperature. Polarizing optical microscopy (POM) experiments were performed using a Leica DM2700P polarization microscope and a Linkam THMS600 hot stage connected to a Linkam T95-PE temperature controller. Phase transition temperatures were determined on cooling at 0.1 °C/min. Differential scanning calorimetry (DSC) measurements were taken using a DSC Q20 V24.11 Build 124. The binary mixtures of CB7CB and RM257 are labeled as "M," followed by a number indicating the concentration of monomer, RM257. Scanning electron microscopy (SEM) images were taken using a Hitachi ultrahigh resolution SU8230 scanning electron microscope. SEM samples were prepared by photopolymerizing the mixtures in planar cells in the desired liquid crystal phase. The liquid crystal and any unreacted monomer were washed out using acetone, leaving behind the aligned polymer network. The washed cells were cracked open and coated with ∼15 nm of conductive carbon.

III. RESULTS AND DISCUSSION

A. Binary mixtures of CB7CB and RM257

The chemical structures of CB7CB and RM257 are given in Fig. 1(a) and the phase diagram of the binary CB7CB/RM257 mixtures (before polymerization) is shown in Fig. 1(b). Initially, as the concentration of RM257 is increased, there is a gradual decrease (by 7 °C) isotropic-nematic transitions (T_{NI}) for concentrations between 0 wt% and 30 wt% RM257. At higher concentrations, T_{NI} increases to 18 °C above the minimum T_{NI}. As the concentration of monomer increases, the N-N_{TB} transition temperature decreases. The N_{TB} phase is seen in mixtures containing up

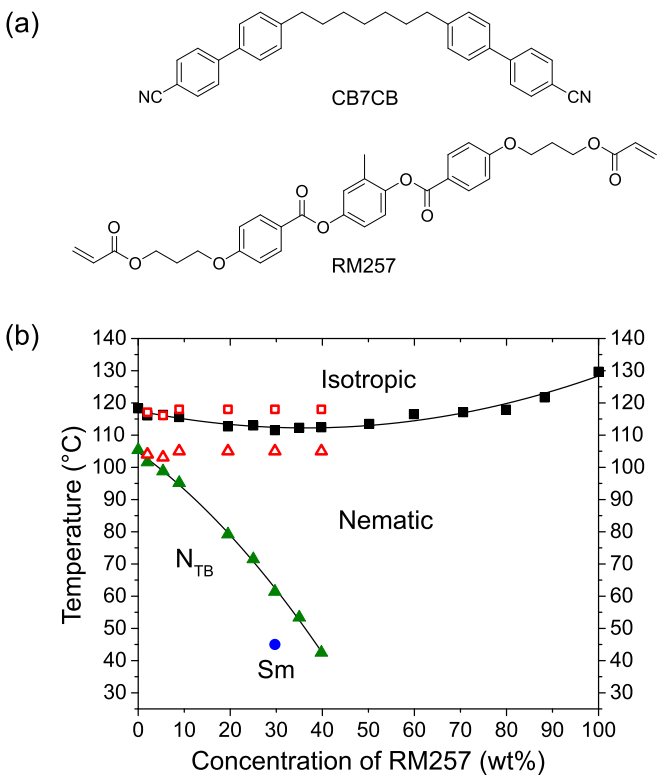

FIG. 1. (a) Chemical structures of molecules CB7CB and RM257. (b) Phase diagram of binary CB7CB/RM257 mixtures before polymerization. Closed symbols represent isotropic-nematic (■), nematic-N_{TB} (▲), and N_{TB} (●) transitions before polymerization. The isotropic, nematic, and N_{TB} regions before polymerization are also labeled. Open symbols represent approximate phase transitions after polymerization (□–T_{NI} and ○–$T_{N\text{-}N_{TB}}$) deduced from changes in birefringence in POM experiments.

to 40 wt% RM257, and at higher concentrations, only the nematic phase is observed (above room temperature). The N_{TB} phases in all unpolymerised CB7CB/RM257 mixtures supercool to room temperature and crystallize within a few hours. The width of the nematic phase increases considerably with increasing monomer concentration, ranging approximately 70 °C at 40 wt% RM257. Interestingly, in the mixture M30 (30 wt% RM257), an additional transition is observed at 45 °C, which corresponds to a transition from the N_{TB} phase to a smectic phase [Figs. 1(b) and 2(c)]. The enthalpy of this N_{TB}-Sm transition is 0.10 kJ/mol. The smectic phase was also observed in mixtures containing 25 wt%, 35 wt%, and 40 wt% of RM257. However, these data points are omitted in the phase diagram in Fig. 1(b), as the N_{TB}-Sm transition was highly second order and determining the exact transition temperature was difficult. Induced smectic phases have previously been observed in binary mixtures of N_{TB} materials [31]; however, although interesting and a possible topic for further investigations, the smectic phase is not the focus of this paper.

The *schlieren* texture of the nematic phase, broken-fan texture of the N_{TB} phase, and focal conic fan texture of the smectic phase of mixture M30 between untreated glass substrates are shown in Fig. 2.

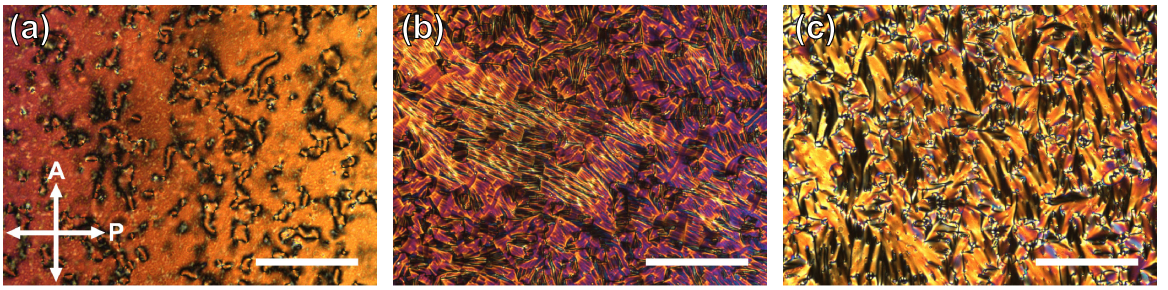

FIG. 2. POM images of M30 between untreated glass substrates: (a) nematic *schlieren* textures at T-$T_{\mathrm{NI}} = -12\,^{\circ}\mathrm{C}$, (b) N_{TB} broken-fan texture at T-$T_{N\text{-}N_{\mathrm{TB}}} = -11\,^{\circ}\mathrm{C}$, (c) smectic focal conics at T-$T_{N_{\mathrm{TB}}\text{-}\mathrm{Sm}} = -11\,^{\circ}\mathrm{C}$. The length of the scale bar is 100 μm. Crossed polarizer "P" and analyzer "A" are labeled.

B. Photopolymerized twist-bend nematic phases

Photopolymerization was carried out on mixtures that exhibited the N_{TB} phase. The samples were contained in homemade planar antiparallel-rubbed cells of 3 μm spacing in their N_{TB} phase and the thermal stability of the polymerized samples was investigated. It was found that when the polymerized samples were left at room temperature, the N_{TB} phase remained stable for the whole period of testing, i.e., several months, compared to the samples before polymerization where the supercooled N_{TB} phases crystallized within a few hours. Also, the N_{TB} phase exists over a temperature range of up to 80 °C (calculated from room temperature to the N-N_{TB} transition). There is very little change in the T_{NI} of the polymerized samples compared to the T_{NI} before polymerization. However, the N-N_{TB} transition temperature in the polymerized samples increases by 2.5 °C in the 2 wt% mixture and by 4.5 °C in the 5.5 wt% mixture.

The behavior of polymerized samples, upon heating from the stable N_{TB} phase is as follows. Polymerized samples with $<$10 wt% monomer show clear textural changes from the ropelike N_{TB} texture at room temperature to the homogeneous nematic texture and subsequently to the isotropic dark texture. Interestingly, above the isotropic transition, residual birefringence is observed in the polymer network. Samples with higher monomer concentration ($\geqslant$10 wt%) also indicate similar interesting characteristics. These are shown in the POM images in Fig. 3 for the polymerized M20 sample. M20 exhibits typical N_{TB} ropelike textures at 25 °C [Fig. 3(a)]. On heating, the birefringence of the sample changes very slightly in the beginning; however, when the sample is heated to temperatures above $\sim$105 °C, there is a noticeable change in birefringence [see Fig. 3(b)]. Further heating results in a more evident decrease in birefringence at temperatures above $\sim$118 °C [Fig. 3(c)]. It should be noted that the temperatures 105 °C and 118 °C are close to the N_{TB}-N and N-Iso transition temperatures in pure CB7CB. Also, as shown in Fig. 3(c), at 120 °C, which is above the isotropic transition temperature of pure CB7CB, the polymer network retains a small residual birefringence. This presence of residual birefringence is true for all photopolymerized N_{TB} mixtures irrespective of the concentration of the monomer. In addition to the residual birefringence, for monomer concentrations $\geqslant$10 wt%, the polymer network also clearly shows the textural features of the N_{TB} phase even above 120 °C [Fig. 3(c)].

The residual birefringence observed in polymerized samples above the liquid crystal's clearing temperature is most likely due to a combination of both the oriented polymer network and induced orientation in the liquid crystal arising at the interface of the liquid crystal and polymer. Such residual birefringence has been reported previously in other polymer stabilized liquid crystals [32,33].

As a comparison, polymerized Sm*A* samples 8CB-RM-10 and 8CB-RM-2 contained in planar cells were tested. The samples 8CB-RM-10 and 8CB-RM-2 are mixtures of 8CB liquid crystal and RM257 monomer in 90 wt%:10 wt% and 98 wt%:2 wt% ratios, respectively. Before polymerization, the mixtures exhibit both the nematic and Sm*A* phases. The nematic to Sm*A* transition before polymerization in the 2% sample is 30.2 °C and in the 10% sample it is 23.1 °C. The mixtures were then polymerized in the Sm*A* phase and heated from room temperature. The POM images of these are given

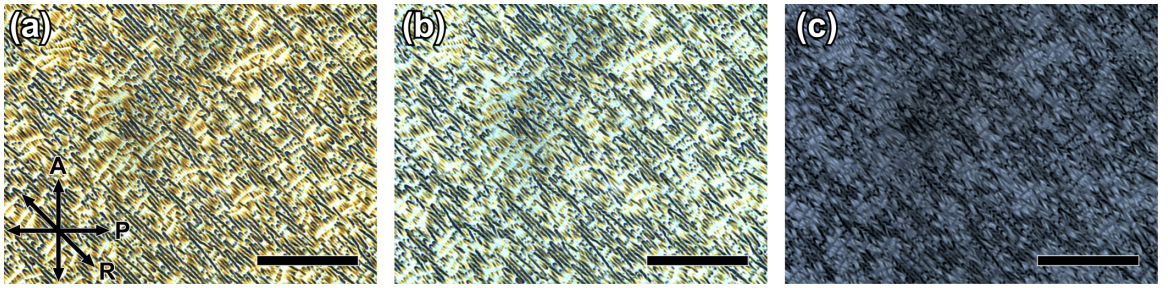

FIG. 3. POM images of the N_{TB} textures of polymerized M20 in a 3-μm planar cell at: (a) 25 °C, (b) 115 °C, (c) 120 °C. R is the rubbing direction and the length of the scale bars is 100 μm. Crossed polarizer "P" and analyzer "A" are labeled.

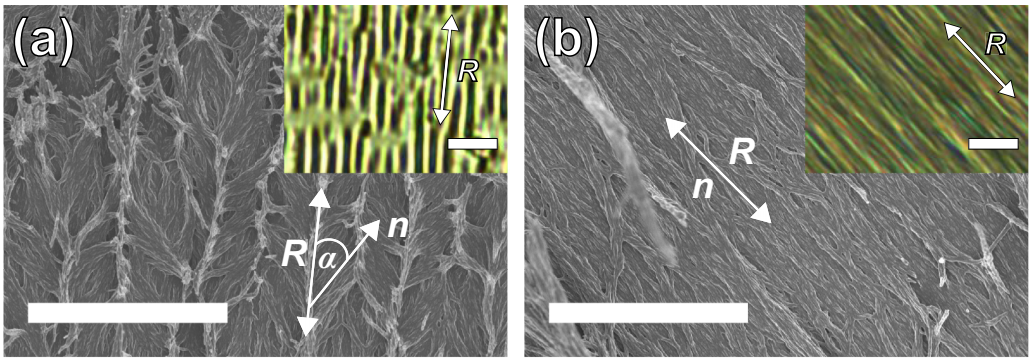

FIG. 4. SEM images of washed samples showing polymer networks of: (a) the N_{TB} phase of polymerized M20, and (b) the Sm*A* phase of polymerized 8CB-RM-10. Corresponding POM images of the phases are provided as insets. The rubbing direction (R) is marked and the length of the scale bars for both the SEM and POM images is 5 μm.

in Fig. S1 of the Supplemental Material [34]. In both polymerized Sm*A* samples, similar behavior to the CB7CB mixtures occurs on heating: (1) a change in birefringence occurs at ∼35 °C, a temperature close to the Sm*A*-*N* transition of pure 8CB, (2) a significant decrease in birefringence is observed at ∼40 °C (which corresponds to the T_{NI} of pure 8CB), and (3) the polymer networks retain the textural features of the Sm*A* phase throughout the entire heating experiment, even above 40 °C. Also, the polymer networks in both the 2% and 10% polymerized Sm*A* samples exhibit residual birefringence above the temperature corresponding to the isotropic transition of the pure liquid crystal, as observed in polymerized N_{TB} samples. The changes in birefringence that appear on heating both the polymerized N_{TB} and Sm*A* samples suggest that the unpolymerized liquid crystals are transitioning to the isotropic state. This transition has been further confirmed by DSC experiments. As summarized in Table S1 (Supplemental Material [34]), two enthalpy peaks are observed in the polymerized M20 sample, which correspond to temperatures at which the N_{TB}-N and N-Iso transitions are observed in pure CB7CB. Likewise, the polymerized 8CB-RM-10 sample shows one transition at 43.6 °C with an associated enthalpy of 0.70 kJ/mol. Even though a clear change in birefringence is observed using POM at ∼35 °C (Fig. S1), a DSC peak corresponding to this transition was not distinguishable (note the small enthalpy of 0.07 kJ/mol associated with the Sm*A*-*N* transition in pure 8CB). For the polymerized 8CB-RM-10 sample, even though a Sm*A*-*N* peak cannot be distinguished in DSC experiments, it can be deduced that there is a transition from the Sm*A* to the N phase, based on changes in birefringence close to the temperature corresponding to the Sm*A* to N transition of pure 8CB. The Sm*A* phase in the 10% sample shows an increase in the width of the Sm*A* phase–before polymerization, the N-Sm*A* transition occurs at 23.1 °C and after polymerization, changes in birefringence occur at ∼35 °C, which is similar to the N-Sm*A* transition of pure 8CB. From (1) the birefringence changes that occurs on heating at temperatures close to the Sm*A*-*N* transition of pure 8CB, (2) the appearance of residual birefringence above the isotropic transition of the pure liquid crystals, and (3) phase transition peaks observed in DSC measurements, it can be concluded that optically, polymerized Sm*A* samples behave similar to the polymerised N_{TB} samples.

Further, to visualize the orientation of polymer strands in the N_{TB} phase, SEM was carried out on the polymerized CB7CB and 8CB samples. The N_{TB} sample was polymerized at T-$T_{N\text{-}N_{TB}} \approx -35$ °C [Fig. 4(a)] and this was then compared with the SEM results of the Sm*A* phase of polymerized 8CB-RM-10 [Fig. 4(b)]. The SEM images in Fig. 4 show well-defined networks of the polymerized mesogen. The corresponding POM images of the N_{TB} and Sm*A* phases are included as insets. In the N_{TB} phase [Fig. 4(a)], the vertical strands in the SEM image are spaced approximately 2 μm apart, which is equivalent to the distance between the stripes in the corresponding POM image. The SEM image shows that the polymer strands form at an angle (α) with respect to the rubbing direction (R). The angle α is approximately 35 ° and this value falls within the reported range [35] of the tilt angle (θ) of CB7CB deduced from birefringence measurements at T-$T_{N\text{-}N_{TB}} \approx -35$ °C. This suggests that the helical axis of the N_{TB} phase lies along the rubbing direction and the polymer strands follow the orientation of the local nematic director $\boldsymbol{n}$ [labeled in Fig. 4(a)]. Therefore, we propose that the angle α [also labeled in Fig. 4(a)] corresponds to the tilt angle θ. This also suggests that photopolymerizing N_{TB} phases at different temperatures below the N-N_{TB} transition could be used as a means of measuring the temperature-dependent N_{TB} tilt angle. In the case of the Sm*A* sample [Fig. 4(b)], the director $\boldsymbol{n}$ lies along the rubbing direction R and the network of polymer strands is clearly aligned parallel to the director.

IV. CONCLUSIONS

In summary, photopolymerization of the twist-bend nematic phase has successfully been employed to form metastable room-temperature N_{TB} phases. In all photopolymerized samples, the N_{TB} phase exists over a temperature range of up to 80 °C. When the polymerized samples are heated, residual birefringence is observed in the polymer network above the isotropic transition of the unpolymerized liquid crystal. SEM imaging of the photopolymerized N_{TB} phase shows that the polymer strands assemble at an angle that corresponds to the tilt angle of the nematic director with respect to the direction of the helical axis. This suggests that photopolymerization of N_{TB} phases could be a means of measuring the tilt angle of the N_{TB} phase.

The data associated with this paper can be found in Ref. [36].

ACKNOWLEDGMENT

N.T. thanks Leeds Anniversary Research Scholarship for funding.

[1] C. Meyer, G. R. Luckhurst, and I. Dozov, Phys. Rev. Lett. **111**, 067801 (2013).
[2] V. P. Panov, R. Balachandran, M. Nagaraj, J. K. Vij, M. G. Tamba, A. Kohlmeier, and G. H. Mehl, Appl. Phys. Lett. **99**, 261903 (2011).
[3] V. P. Panov, M. Nagaraj, J. K. Vij, Y. P. Panarin, A. Kohlmeier, M. G. Tamba, R. A. Lewis, and G. H. Mehl, Phys. Rev. Lett. **105**, 167801 (2010).
[4] D. Chen, J. H. Porada, J. B. Hooper, A. Klittnick, Y. Shen, M. R. Tuchband, E. Korblova, D. Bedrov, D. M. Walba, M. A. Glaser, J. E. Maclennan, and N. A. Clark, Proc. Natl. Acad. Sci. USA **110**, 15931 (2013).
[5] M. Cestari, S. Diez-Berart, D. A. Dunmur, A. Ferrarini, M. R. de la Fuente, D. J. B. Jackson, D. O. Lopez, G. R. Luckhurst, M. A. Perez-Jubindo, R. M. Richardson, J. Salud, B. A. Timimi, and H. Zimmermann, Phys. Rev. E **84**, 031704 (2011).
[6] Z. Zhang, V. P. Panov, M. Nagaraj, R. J. Mandle, J. W. Goodby, G. R. Luckhurst, J. C. Jones, and H. F. Gleeson, J. Mater. Chem. C **3**, 10007 (2015).
[7] R. J. Mandle, E. J. Davis, C. T. Archbold, S. J. Cowling, and J. W. Goodby, J. Mater. Chem. C **2**, 556 (2014).
[8] Y. Wang, G. Singh, D. M. Agra-Kooijman, M. Gao, H. K. Bisoyi, C. Xue, M. R. Fisch, S. Kumar, and Q. Li, CrystEngComm **17**, 2778 (2015).
[9] R. J. Mandle and J. W. Goodby, RSC Adv. **6**, 34885 (2016).
[10] S. P. Sreenilayam, V. P. Panov, J. K. Vij, and G. Shanker, Liq. Cryst. **44**, 244 (2017).
[11] D. Chen, M. Nakata, R. Shao, M. R. Tuchband, M. Shuai, U. Baumeister, W. Weissflog, D. M. Walba, M. A. Glaser, J. E. Maclennan, and N. A. Clark, Phys. Rev. E **89**, 022506 (2014).
[12] N. Trbojevic, D. J. Read, and M. Nagaraj, Phys. Rev. E **96**, 052703 (2017).
[13] A. A. Dawood, M. C. Grossel, G. R. Luckhurst, R. M. Richardson, B. A. Timimi, N. J. Wells, and Y. Z. Yousif, Liq. Cryst. **43**, 2 (2016).
[14] D. M. Walba, Science **270**, 250 (1995).
[15] I. Dierking, Adv. Mater. **12**, 167 (2000).
[16] I. Dierking, Materials **7**, 3568 (2014).
[17] D. J. Broer, J. Boven, G. N. Mol, and G. Challa, Makromol. Chem. **190**, 2255 (1989).
[18] R. A. M. Hikmet, J. Lub, and J. A. Higgins, Polymer **34**, 1736 (1993).
[19] P. Archer and I. Dierking, Soft Matter **5**, 835 (2009).
[20] H. Kikuchi, M. Yokota, Y. Hisakado, H. Yang, and T. Kajiyama, Nat. Mater. **1**, 64 (2002).
[21] H. J. Coles and M. N. Pivnenko, Nature **436**, 997 (2005).
[22] D. J. Broer, J. Lub, and G. N. Mol, Nature **378**, 467 (1995).
[23] J. Guo, H. Cao, J. Wei, D. Zhang, F. Liu, G. Pan, D. Zhao, W. He, and H. Yang, Appl. Phys. Lett. **93**, 201901 (2008).
[24] A. Varanytsia and L.-C. Chien, J. Appl. Phys. **119**, 014502 (2016).
[25] I. Dierking, L. Komitov, S. T. Lagerwall, T. Wittig, and R. Zentel, Liq. Cryst. **26**, 1511 (1999).
[26] C. A. Guymon, E. N. Hogga, D. M. Walba, N. A. Clark, and C. N. Bowman, Liq. Cryst. **19**, 719 (1995).
[27] H. Fujikake, H. Sato, and T. Murashige, Displays **25**, 3 (2004).
[28] A. Labeeb, H. F. Gleeson, and T. Hegmann, Appl. Phys. Lett. **107**, 232903 (2015).
[29] J. Strauss and H. -S. Kitzerow, Appl. Phys. Lett. **69**, 725 (1996).
[30] V. P. Panov, S. P. Sreenilayam, Y. P. Panarin, J. K. Vij, C. J. Welch, and G. H. Mehl, Nano Lett. **17**, 7515 (2017).
[31] A. Knežević, I. Dokli, M. Sapunar, S. Šegota, U. Baumeister, and A. Lesac, Beilstein J. Nanotechnol. **9**, 1297 (2018).
[32] T. Sergan, I. Dozov, V. Sergan, and R. Voss, Phys. Rev. E **95**, 052706 (2017).
[33] R. A. M. Hikmet, Liq. Cryst. **9**, 405 (1991).
[34] See Supplemental Material at http://link.aps.org/supplemental/10.1103/PhysRevE.99.062704 for (1) POM images of polymerised SmA samples 8CB-RM-2 and 8CB-RM-10 on heating from room temperature and (2) enthalpy of phase transitions for pure and polymerised liquid crystals.
[35] C. Meyer, G. R. Luckhurst, and I. Dozov, J. Mater. Chem. C **3**, 318 (2015).
[36] https://doi.org/10.5518/602.